International Journal of Nanomedicine

Dovepress
Taylor & Francis Group

Open Access Full Text Article

ORIGINAL RESEARCH

Microfluidic Synthesis of miR-200c-3p Lipid Nanoparticles: Targeting ZEB2 to Alleviate Chondrocyte Damage in Osteoarthritis

Dong Zheng[1,*], Tong Chen[2,*], Kaiyuan Yang[1], Guangrong Yin[1], Yang Chen[3], Jianchao Gui[4], Chao Xu[1], Songwei Lv[5]

[1]Department of Orthopedics, The Affiliated Changzhou No.2 People's Hospital with Nanjing Medical University, The Third Affiliated Hospital of Nanjing Medical University, Changzhou, People's Republic of China; [2]Department of Orthopedics, The First Affiliated Hospital of Nanjing Medical University, Nanjing, People's Republic of China; [3]Changzhou Productivity Development Center, Changzhou, People's Republic of China; [4]Department of Sports Medicine and Joint Surgery, Nanjing First Hospital, Nanjing Medical University, Nanjing, People's Republic of China; [5]School of Pharmacy, Changzhou University, Changzhou, People's Republic of China

*These authors contributed equally to this work

Correspondence: Chao Xu; Songwei Lv, Email xuchao_06@163.com; lvsw@cczu.edu.cn

Introduction: Osteoarthritis (OA) is a degenerative joint disease characterized by articular cartilage degeneration. Chondrocyte inflammation, apoptosis, and extracellular matrix degradation accelerated OA progression. MicroRNA (miRNA) has the potential to be a therapeutic method for osteoarthritis. However, it is difficult to penetrate the cell to exercise its biological function, and its extracellular effect is unclear.

Methods: lipo-AgPEI-miR-200c-3p was created by combining miR-200c-3p with silver nitrate polyvinylimine nanoparticles on a microfluidic device. The drug release curve, stability, temperature sensitivity, cytotoxicity, and the impact of lipo-AgPEI-miR-200c-3p on the expression of proteins linked to matrix disintegration, apoptosis, and inflammatory factors were all detected.

Results: Results showed that the particle size of Lipo-AgPEI-miR-200c-3p was about 130 nm, the Zeta potential was lowered to 1.08 ±0.12 mV. Lipo-AgPEI-miR-200c-3p could increase cell viability, prevent cell apoptosis, and decrease the expression levels of TNF-α, IL-6, IL-1β, and MCP-1 in ADTC5 cells following LPS stimulation. MMP3, MMP13, and ADAMTS-4 expression was downregulated whereas collagen II expression was upregulated. The ZEB2 expression was greatly elevated following LPS stimulation and dramatically decreased following transfection of miR-200c-3p. Collagen II expression rose following transfection of si-ZEB2, whereas the expression levels of inflammatory factors, apoptosis-related proteins, MMP3, MMP13, and ADAMTS-4 decreased. The dual luciferase experiment demonstrated that ZEB2 was the target gene of miR-200c-3p.

Conclusion: The synergistic effect of AgPEI and miR-200c-3p can inhibit the inflammatory response, apoptosis, and matrix degradation of chondrocytes. Lipo-AgPEI-miR-200c-3p can also improve transfection efficiency and obtain good physicochemical properties of drugs. miR-200c-3p may be crucial in the development of OA and can influence the target gene ZEB2, control the inflammatory response, apoptosis, and chondrocyte matrix breakdown.

Keywords: microfluidic synthesis, miR-200c-3p, lipid nanoparticles, osteoarthritis, ZEB2

Introduction

With the greatest rate of impairment among chronic diseases of aging, osteoarthritis (OA) is the most frequent kind of arthritis and can raise the risk of disability in older persons.[1–4] Slowly but surely, osteoarthritis is getting more common as the population ages and is starting to pose a serious threat to older adults' health. Joint discomfort is the most common clinical characteristic of OA patients, which leads to restricted activity and joint pain.[1] Sleep difficulties are very common, and they have a major negative impact on patients' quality of life. Drug therapy is the primary clinical treatment used to treat OA today, with the goal of enhancing patient quality of life and minimizing pain. Opioids, non-steroidal anti-inflammatory medications,

Received: 17 September 2024
Accepted: 21 December 2024
Published: 14 January 2025

and other analgesics are the most often utilized medications.[5–7] Although studies have demonstrated that opioids are helpful in relieving pain, they are unable to reduce the likelihood of impairment or the necessity for surgery. Furthermore, using opioids frequently raises the possibility of abusing them, which can have detrimental side effects like nausea, constipation, dizziness, sleepiness, and addiction. NSAIDs' pharmacological actions make them useful for antipyretic, analgesic, and anti-inflammatory purposes; nevertheless, prolonged oral NSAID use can result in side effects such renal damage and gastrointestinal bleeding.[8] On the other hand, because of the characteristics of OA, patients frequently need to take medications for an extended period of time. Because OA patients are unique, dose and individual medication monitoring should receive more consideration.

As research progressed, treatments for osteoarthritis (OA) such as gene therapy, biological agent application, and stem cell injection into the articular cavity were introduced. Gene therapy is the process of transfecting target genes into specific cells to enable them to function.[9–11] However, it is required to design a variety of effective carrier materials for gene delivery because pure naked genes are easily broken down by several biological enzymes in the body during the process of in-body transmission and lose their life activities, leading to poor therapeutic impact.[12] Research has demonstrated that various carrier materials frequently have a significant influence on the effectiveness of gene transfer and transfection, which in turn determines the therapeutic outcome. Currently, gene vectors are mostly classified as viral or non-viral based on compositional differences.[13–15] High delivery efficiency and some success in clinical trials have been attained via viral vector. At present, it's the most researched and efficient carrier material available. Nevertheless, the virus vector may pose a risk to public health due to immune response, easily mutated genes, etc. The health of the patients is much at stake due to these possible safety issues. The virus vector also has certain drawbacks, including high production costs, a difficult preparation procedure, a low gene load, immunogenic reactions, and carcinogenesis. While non-viral vectors can compensate for the shortcomings of the aforementioned viral vectors, they frequently have poorer transfection and distribution efficiencies than viral vectors.[16,17]

Studies have shown that miRNA can effectively control inflammation and play an important role in chondrocyte proliferation, apoptosis, autophagy, hypertrophy and regulation of extracellular matrix degradation.[18–21] However, miRNAs are easily degraded by extracellular ribonuclease, so they need to be efficiently delivered to target cells through related vectors.[22–24] Duan et al found that miR-140 inhibited IL-1β and MMP expression by regulating the BMP2 and TGFBR expression in OA chondrocytes.[25] miR-34a could inhibit fibroblast-like synoviocytes (FLSs) apoptosis by regulating TGIF2.[26] Overexpression of miR-93-5p could inhibit the inflammatory response and apoptosis in OA articular chondrocytes.[27] microRNA-224-5p could protect articular cartilage from degeneration and further synthesize urchin-like ceria nanoparticles (NPs) that can load miR-224-5p for enhanced gene therapy of OA.[28] However, the mechanism of action of miR-200c-3p on chondrocyte damage remain unclear.[29]

Furthermore, research has shown that medications that combine metal ions (such as magnesium, silver, zinc, etc.) to create nanoparticles are effective in treating rheumatoid arthritis and osteoarthritis.[30,31] Silver nanoparticles have the effect of regulating apoptosis and anti-inflammatory activities.[32–35] Silver nanoparticles modified with polyethylene glycol (PEG) could deliver folic acid, induce apoptosis in M1 macrophages, promote M2 macrophages polarization, and inhibit RA progress.[36] Therefore, whether gene carrier drugs can be designed to use silver nanoparticles to carry miRNA to treat the inflammatory response of chondrocytes in OA has become the original intention and scientific hypothesis of our experimental research design.

This study aims to comprehensively determine the effects and biological mechanism of Lipo-AgPEI-miR-200c-3p nanoparticles on chondrocyte damage. In this study, Lipo-AgPEI-miR-200c-3p nanoparticles synthesized by microfluidic microchips. The particle size, morphology, stability, cytotoxicity and phase transition temperature of Lipo-AgPEI-miR-200c-3p were characterized. Liposome encapsulation can reduce the cytotoxicity of gene delivery vector materials, improve transfection efficiency, and obtain good physicochemical properties of drugs[19,37] Simultaneously, the function and molecular mechanism of miR-200c-3p were investigated in relation to the LPS-mediated inflammatory response, apoptosis, and matrix degradation of mouse ATDC5 cells. Additionally, the database was utilized to predict the downstream target genes of this protein. Furthermore, target genes were knocked down via small interfering RNA (siRNA) to investigate their regulatory impact on ATDC5 cell proliferation and cell cycle, as well as their capacity to prevent inflammation, apoptosis, and extracellular matrix disintegration. In

an effort to find new targets for the treatment of OA, dual luciferase reports confirmed the relationship between miR-200c-3p and its downstream target genes.

Materials and Methods

Materials

Branched polyethyleneimine (B-PEI, Mn=10000) was purchased from Sigma-Aldrich Company. N-2-hydroxyethylpiperazine-N′-2-ethanesulfonic acid (HEPE) was purchased from Aladdin Reagent Company. Shanghai AVT Pharmaceutical Technology Co., Ltd. supplied the cholesterol, distearoylphosphatidyl ethanolamine-polyethylene glycol (DSPE-PEG2000), and dipalmitoylphosphatidylcholine (DPPC). Adamas Reagent Company provided the silver nitrate ($AgNO_3$). The CCK-8 kit (C0038), BCA protein concentration kit (P0012), IL-1β Elisa kit (PI301), IL-6 Elisa kit (PI326), TNF-α Elisa kit (PT512) and MCP-1 Elisa kit (PC125) were purchased from Beyotime Reagent Company. Cell Signaling Technologies (CST) provided the bcl2 (3498S), cleaved caspase3 (9661S), caspase3 (9662S), and anti-rabbit IgG (7074P2) antibodies. ADAMTS-4 (ab185722) and MMP3 (ab52915) antibodies were supplied from Abcam. Proteintech Group was the source of MMP13 (18,165-1-AP) and Collagen II (28549-1-AP) antibodies. Beijing Boosen Biotechnology Co., LTD was the supplier of GAPDH (bs-2188R). Every reagent was purchased from commercial vendors and was of analytical grade, requiring no additional purification.

Preparation of AgPEI-miR-200c-3p Nanoparticles

Dissolve 40 mg $AgNO_3$ powder in 10 ml deionized water, add it drop by drop into 20 mg/mL B-PEI solution (mass ratio B-PEI: $AgNO_3$=10:1), stir away from light for 45 minutes. The above solution should be immersed in 90 °C oil bath for about 1 hour, stop heating when the solution appears white turbid color, cool to room temperature, dilute the solution 10 times and store for later use. The miR-200c-3p was dissolved in 125μL DEPC solution, and the disinfected Hepes buffer was added with 375μL, and the miR-200c-3p solution was dissolved by oscillating dispersion. Take 127μL of sterilized AgPEI solution, add 373μL of sterilized Hepes buffer, shake the Hepes buffer after adding 373μl of sterilized Hepes buffer, and shake the solution to dissolve. AgPEI-miR-200c-3p solution was prepared by adding miR-200c-3p solution and dispersing it with eddy current mixer for 30 seconds and standing at room temperature for 30 minutes.

Preparation and Characterization of Liposome Nanoparticle Lipo-AgPEI-miR-200c-3p

As part of the A solution (methanol phase), DPPC, cholesterol, and DSPE-PEG2000 were combined with methanol. PBS solution was used as B solution (aqueous phase) to disperse the AgPEI-miR-200c-3p solution that was previously made. Subsequently, both solution A and solution B were simultaneously injected into the micromixer (Figure S1), resulting in a silver nanoparticle solution that contained miR-200c-3p liposomes (Lipo-AgPEI-miR-200c-3p). Initial lipid concentrations for each formulation were 4 mg/mL, water-organic flow rate ratios (FRR) were 4:1, and total flow rates (TFR) were 25 mL/min.

The morphology of Lipo-AgPEI-miR-200c-3p nanoparticles was observed by JEOL JEM-2010 TEM at 100KV acceleration voltage. The size distribution of Lipo-AgPEI-miR-200c-3p nanoparticles was measured using dynamic light scattering (DLS) (Zetasizer Nano-ZS 90, Malvern). The phase transition temperature of Lipo-AgPEI-miR-200c-3p nanoparticles was determined by differential scanning calorimeter (Diamond DSC). The Lipo-AgPEI-miR-200c-3p nanoparticles were stored in a refrigerator at 4 °C, and some of them were tested for particle size at regular intervals to analyze their stability.

Chondrocyte Culture and Establish Osteoarthritis Model in vitro

The ATDC5 cell line (Mouse chondroblast) was obtained from China Center for Type Culture Collection. ATDC5 cells were cultured in DMEM F/12 medium containing 10% fetal bovine serum (FBS, Gibco), 100 U/ml penicillin (Gibco), and 0.1 mg/mL streptomycin (Gibco). When the cell reached 70%, cells were treated with 350 μg/mL LPS for 6 h, 12 h, and 24 h to induce osteoarthritis chondrocyte model.

Determination of Materials Toxicity by MTS

The cytotoxicity of PEI, Ag ($AgNO_3$), Ag-PEI, AgPEi-miR-200C-3p, and Lipo-AgPEI-miR-200c-3p were determined by MTS. ATDC5 cells were seeded in 96-well plates at a density of 5000 cells per well and cultured with DMEM F/12 medium for 24h. Subsequently, 10μL MTS solution was added to each well and incubated for 4 h. Then, removed the supernatant and the absorbance at 490 nm was determined by microplate reader (Elx808™ Bio-Tek Instruments, Winooski, VT, USA).

Encapsulation Rate and Release Rate of miR-200c-3p

Dynamic membrane dialysis was used to evaluate the release degree of Lipo-AgPEI-miR-200c-3p nanoparticles in vitro. Lipo-AgPEI-miR-200c-3p nanoparticles were carefully weighed and put in a dialysis bag together with the release medium phosphate buffer solution (pH 7.0), using the original AgPEI-miR-200c-3p solution (33 μg/mL estimated according to miR-200c-3p) as the control. Each dialysis bag had a 1 mL liquid capacity. After sealing the bag, it was placed into the centrifuge tube. After being incubated in a constant temperature shaker at 80 r/min and 37 °C, 1 mL of the AgPEI-miR-200c-3p solution was taken out of a centrifuge tube at various intervals, and the same volume of buffer was added.

RT-qPCR Analysis

Total RNA isolation was carried out using the NucleoSpin RNA Kit (MN, Düren, Germany) according to the manufacturer's instructions. Subsequently, cDNA synthesis was performed utilizing the High-Capacity cDNA Reverse Transcription Kit (Applied Biosystems, Foster City, CA, USA) following the manufacturer's recommended protocols. RT-qPCR analysis was conducted employing the using SYBR™ Select Master Mix (Applied Biosystems, Austin, TX, USA) on the CFX96™ Real-Time PCR Detection Systems (Bio-Rad, USA). Primer sequences, designed by Shenggong Biotech. Co., Ltd. (Shanghai, China) were listed in Table 1. The expression level was determined based on the threshold cycle (Ct), and relative expression levels were analyzed by $2^{-\Delta\Delta CT}$. Primer sequences of other genes are shown in Table S1.

Elisa Analysis

The cell culture supernatant was extracted and the protein expression was detected by Elisa kits according to the manufacturer's instructions. The optical density (OD) at 450 nm was determined by microplate reader (Elx808™ Bio-Tek Instruments, Winooski, VT, USA).

Tunel Assay

2×10^4 ATDC5 cells were seeded onto the slide and cultivated for 24 h, then stimulated following experimental conditions. After the end of the intervention, the cell apoptosis was detected with Tunel Imaging Kits (40306ES60; Yisheng Biotechnology Co., Ltd., Shanghai, China) according to the manufacturer's instructions. The results were analyzed using Image J software (Tree Star, Inc., USA).

Flow Cytometry

ATDC5 cells were transfected with si-RNA and treated with LPS. After treatment, the chondrocytes were harvested and washed with PBS and then resuspended in 100 μL binding buffer. FITC Annexin V and propidium iodide (PI) were added for 10 min at room temperature without light. After cultivation, the 400 μL binding buffer was added, and the cells were analyzed with a FACScan flow cytometer (BD Biosciences, San Jose, CA, USA). The results were analyzed with FlowJo software (Tree Star, Inc., USA).

Table 1 miR-200c-3p and U6 primer sequences.

Gene	Upstream Primer	Downstream Primer
miR-200c-3p	AATACTGCCGGGTAATGATGGA	CTCTACAGCTATATTGCCAGCCAC
U6	CTCGCTTCGGCAGCACA	AACGCTTCACGAATTTGCGT

Western Blot Analysis

ATDC5 cells at the logarithmic growth stage were seeded into 6-well plates at a density of 2×10^5 per well, and plasma envelope proteins were extracted 48 hours later. The progress of western blot was described in the previous study.[38] All samples were analyzed by SDS-PAGE and transferred to PVDF membrane (Merck Millipore, USA). All antibody information is described in the Materials section. Image J software was used to evaluate the expression of relative proteins and GraphPad Prism software was used to perform experimental data.

Bioinformatics Analysis of Online Databases

TargetScan databases: TargetScan databases (http://www.targetscan.org/) search for a match with the seeds of the miRNA sequences of conservative killing 8 killing, killing 7 and 6 loci to predict the miRNA biological targets. miRDB database (http://mirdb.org/) predicts miRNA targets by calculating common features associated with miRNA binding and down-regulation using machine learning methods.

Statistical Analysis

At least three independent biological replicates were conducted for each experiment, the data were expressed as mean ± standard deviation (SD). Unpaired Student's *t*-test was used for two groups. One-way ANOVA and the Tukey test were used to analyze the differences between the multiple groups. $*P<0.05$, $**P < 0.01$, $***P < 0.001$ were considered statistically significant.

Results

Synthesis of Lipo-AgPEI-miR-200c-3p Nanoparticles

As shown in Figure 1A, we prepared polyethylenimide (PEI) nanoparticle drugs by taking advantage of the positive charge on the surface of non-viral gene carrier PEI, small particle size, ease of cell endocytosis, and benefits of small-molecular weight branched-chain PEI that can carry more gene fragments. Following the formation of AgPEI nanoparticles by the complex of metal silver ions with branched-chain PEI, AgPEI-miR-200c-3p nanoparticles were produced by loading miR-200c-3p. Second, a liposome-based drug delivery system that was appropriate for AgPEI-miR-200c-3p was developed. AgPEI-miR-200c-3p was then coated with nano-liposomes made from ethanolamine-polyethylene glycol (DSPE-PEG2000), a mixture of PEG, cholesterol, and phospholipid (Figure 1D). AgPEI-miR-200c-3p and AgPEI polymers were both discovered to have nanoscale particle sizes by electron microscopy, with AgPEI-miR-200c-3p exhibiting slightly larger particle sizes than AgPEI (Figure 1B-1C). The average particle size of AgPEI nanoparticles is 44.4 nm and the dispersion coefficient PDI is 0.312 by using DLS, while the average particle size of AgPEI-miR-200c-3p nanoparticles is 47.6 nm and the dispersion coefficient PDI is 0.350 (Figure 1). The Zeta potential of AgPEI was 35.3 ±0.36 mV, while the Zeta potential of AgPEI-miR-200c-3p obtained by adsorption of miR-200c-3p decreased to 10.4 ±0.22 mV, with statistical significance ($*P<0.05$) (Figure S2).

To optimize Lipo-AgPEI-miR-200c-3p preparation, various flow rate ratios (FRR) and total flow rates (TFR) were studied. As shown in Figure 1F, with the flow rate ratio of 1:1 rising to 6:1, the particle size of the liposome prepared gradually decreased from 169 nm to 103 nm. Considering the particle size and uniformity (PDI) comprehensively, the flow rate ratio was 3:1 for subsequent tests. Under the condition of a fixed flow rate ratio of 3:1, the total flow rate was continued to be explored. It can be seen from Figure 1G that as the total flow rate keeps rising, the particle size of the prepared liposomes keeps decreasing and the PDI gradually increases. Considering the particle size and uniformity, the total flow rate was fixed at 15 mL/min: 3 mL/min. According to TEM imaging, Lipo-AgPEI-miR-200c-3p had particles that were roughly 120 nm in size, which was in line with the findings of DLS (Figure 1E). The entire Lipo-AgPEI-miR -200c-3p nanoparticle was spherical or sphere-like, and the AgPEI-miR-200c-3p nanoparticles were well enclosed within the liposome. Compared to AgPEI-miR-200c-3p, Lipo-AgPEI-miR-200c-3p had a substantially lower average Zeta potential of 1.08± 0.12mV, as determined by DLS (Figure S2). Furthermore, after seven days of storage, the particle size and PDI did not significantly increase, indicating that the Lipo-AgPEI-miR-200c-3p were stable (Figure 1H). The transition temperature of Lipo-AgPEI-miR-200c-3p was displayed in the DSC calorimetric profiles (Figure 1I). To

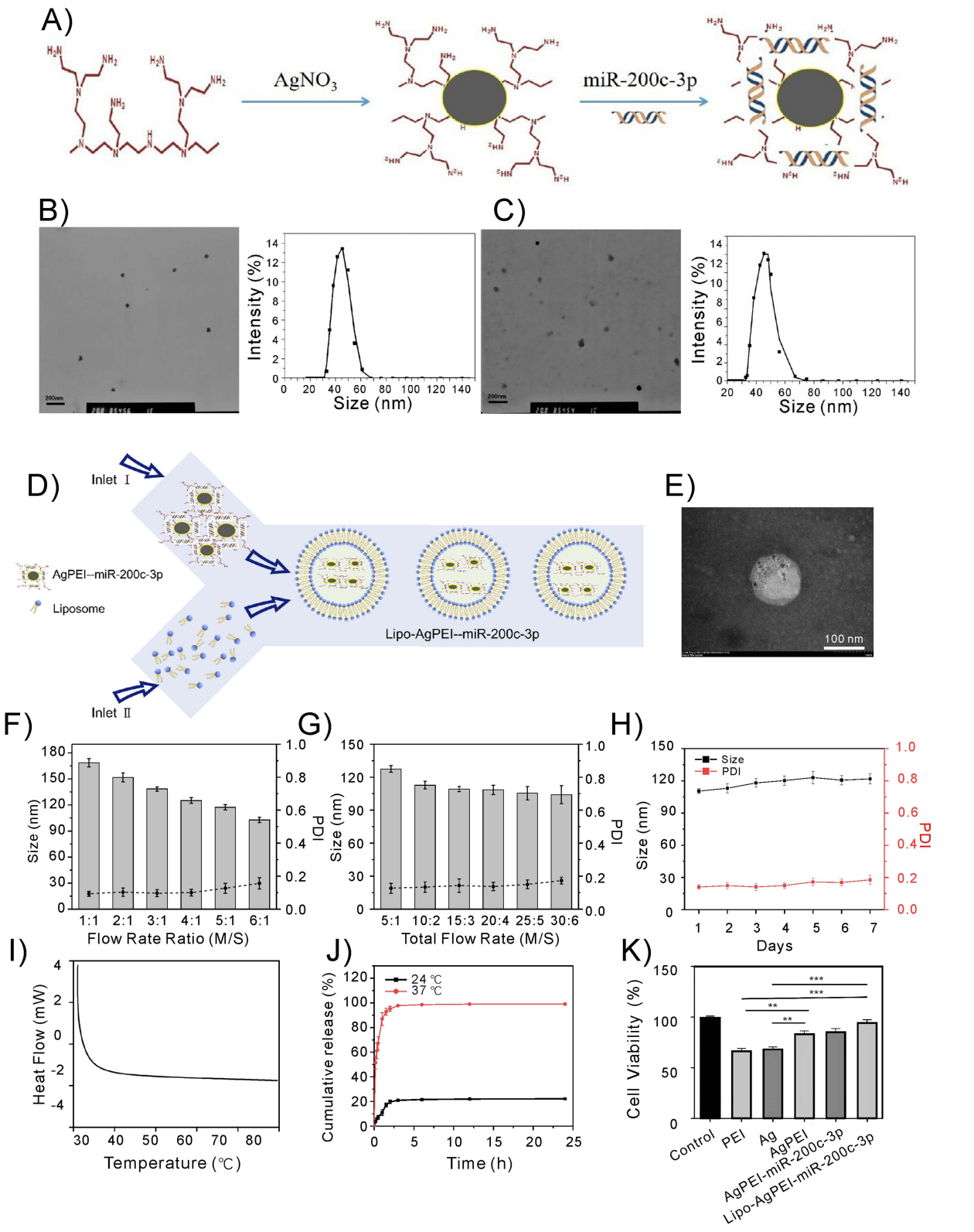

Figure 1 Characteristics of the AgPEI-miR-200c-3p and preparation of Lipo-AgPEI-miR-200c-3p. (**A**) Schematic diagram of preparation of AgPEI-miR-200c-3p. (**B**) TEM and DLS images of Ag-PEI. (**C**) TEM and DLS images of AgPEI-miR-200c-3p. (**D**) A schematic illustration of the one-step microfluidic fabrication of Lipo-AgPEI-miR-200c-3p. (**E**) TEM image of Lipo-AgPEI-miR-200c-3p. (**F**) Effect of different flow rate ratios on Lipo-AgPEI-miR-200c-3p size and PDI. M/S: Methanol phase/ aqueous phase. (**G**) Effect of different total flow rates on Lipo-AgPEI-miR-200c-3p size and PDI. (**H**) Stability analysis of Lipo-AgPEI-miR-200c-3p. (**I**) DSC curve of Lipo-AgPEI-miR-200c-3p. (**J**) Temperature-controlled AgPEI-miR-200c-3p release from Lipo-AgPEI-miR-200c-3p. (**K**) The cell viability of Lipo-AgPEI-miR-200c-3p. Statistical significance was determined by one-way ANOVA. $^{**}P < 0.01$, $^{***}P < 0.001$.

investigate the release regularity of Lipo-AgPEI-miRNA-200c-3p at varying temperatures, the Lipo-AgPEI-miRNA -200c-3p was subjected to phosphate buffers at 24 °C and 37 °C, respectively, to measure the release quantity across varying time intervals. These results indicated that liposomes could play a function of slow release with intelligent response to temperature, and effectively control miRNA to reach the lesion area (Figure 1J). RT-qCR results showed that compared with AgPEI-miR-200c-3p, the expression of miR-200c-3p in Lipo-AgPEI-miR-200c-3p in transfection group was significantly increased (Figure S3).

The Cell Viability of Lipo-AgPEI-miR-200c-3p

Figure 1K illustrates that Lipo-AgPEI-miR-200c-3p has no significant effect on cell viability and that its cytotoxicity differs significantly from that of pure PEI and Ag groups. $AgNO_3$ and linear L-PEI both show some cytotoxicity. Silver nitrate and branched-chain B-PEI combine to generate AgPEI nanoparticles, which effectively lower the material's cytotoxicity. After miR-200c-3p is loaded into AgPEI-miR-200c-3P nanoparticles, the cytotoxicity varies, although not significantly. The material's toxicity can be effectively inhibited by the good biocompatibility of nano-liposome microlipo-AgPEI-miR-200c-3p.

Lipo-AgPEI-miR-200c-3p Reversed Cell Viability Treated by LPS in ATDC5 Cells

ATDC5 cells were treated with 350 μg/ mL LPS for 6h, 12h, and 24 h, respectively. The CCK8 results showed that with the increase of time, cell viability and expression of miR-200c-3p were gradually decreased, and cell viability significantly decreased after LPS treatment for 12 h and 24 h (Figure 2A and C). Therefore, the 350 μg/mL LPS were selected to treat chondrocytes for 24h to induce osteoarthritis cell model. The level of miR-200c-3p was significantly decreased when ATDC5 cells were treated with LPS. Meanwhile, the expression of miR-200c-3p was significantly increased after transfecting the Lipo-AgPEI-miR-200c-3p. The CCK8 results showed that the cell viability decreased significantly after LPS treatment. When cells were transfected with miR-200c-3p and treated with LPS or added AgPEI, cell viability was increased compared with that after LPS treatment (Figure 2B). After being treated with LPS and transfected with miR-200c-3p by adding Lipo-AgPEI-miR-200c-3p, the cell activity was increased compared with that of the LPS+miR-NC group (Figure 2D). The results showed that miR-200c-3p delivered via Lipo-AgPEI-miR-200c-3p could effectively reverse LPS-induced cell viability.

Lipo-AgPEI-miR-200c-3p Inhibited ATDC5 Cells Apoptosis

Tunel staining results indicated that chondrocytes were transfected with miR-200c-3p or treated with AgPEI could partly inhibit chondrocyte apoptosis induced by LPS. Interestingly, when chondrocytes were transfected with Lipo-AgPEI-miR-200c-3p, chondrocyte apoptosis levels were further decreased (Figure 3A and C). The balance of anti-apoptotic protein Bcl-2 and pro-apoptotic protein Bax / cleaved caspase3 plays an important role in regulation of cell survival. Western blot results showed that the expression of pro-apoptotic factors Bax and cleaved caspase3 were up-regulated, and the expression of anti-apoptotic factor Bcl-2 was down-regulated in LPS groups. Bax and cleaved caspase-3 showed considerably lower expression levels after being treated with LPS and then transfected with miR-200c-3p or supplemented with AgPEI, however anti-apoptotic factor Bcl-2 showed higher expression. Moreover, transfected miR-200c-3p with Lipo-AgPEI-miR-200c-3p significantly upregulated Bcl2 expression while downregulated Bax and cleaved caspase3 expression (Figure 3B, D–F and Figure S4). These findings suggested that the delivery of miR-200c-3p via Lipo-AgPEI-miR-200c-3p could more successfully inhibit chondrocyte apoptosis.

Lipo-AgPEI-miR-200c-3p Suppressed ATDC5 Cells Inflammation and Cartilage Degradation

To further explore the role of miR-200c-3p on LPS-induced ATDC5 cells' inflammatory response, multiple inflammatory factors were detected by Elisa. The results showed that the TNF-α, IL-6, IL-1β and MCP-1 expressions were increased significantly after LPS treatment and dramatically decreased when treated with AgPEI or transfected with the miR-200c-3p,

 https://doi.org/10.2147/IJN.S491711

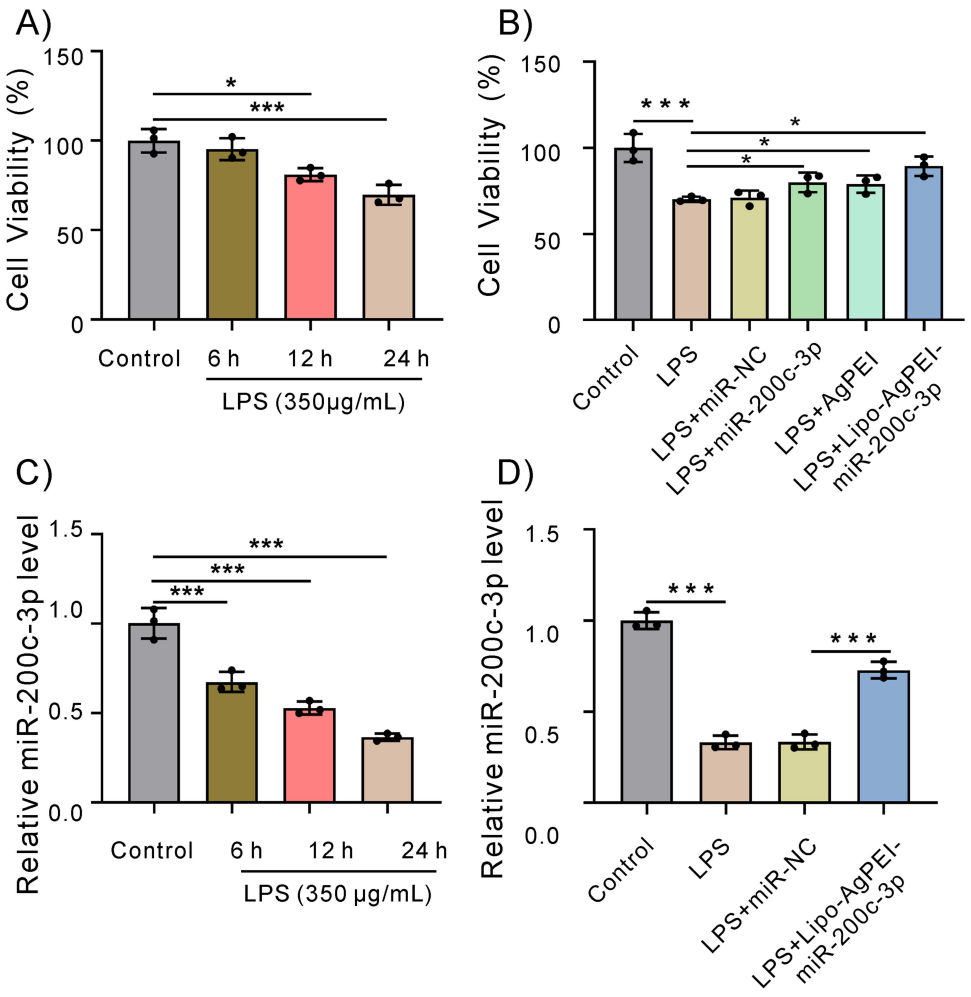

Figure 2 Effects of LPS on ATDC5 cells viability and the expression level of miR-200c-3p. (**A**) The ADTC5 cells were stimulated by LPS and cell viability was detected by CCK-8 at different times. (**B**) The impact of Lipo-AgPEI-miR-200c-3p delivering miR-200c-3p on ATDC5 cell viability was determined using CCK-8. (**C**) The ADTC5 cells were stimulated by LPS and the expression of miR-200c-3p was detected by RT-qPCR. (**D**) The expressions of miR-200c-3p were detected by RT-qPCR after transfecting miR-200c-3p with Lipo-AgPEI-miR-200c-3p and then treated with LPS. Data are representative of three independent experiments and presented as means ± SD. Statistical significance was determined by one-way ANOVA. *$P < 0.05$, ***$P < 0.001$.

which indicated that AgPEI and miR-200c-3p overexpression could be able to partially mitigate the inflammatory response caused by LPS. Interestingly, pro-inflammatory factor levels were dramatically decreased after treating Lipo-AgPEI-miR-200c-3p, when compared with the LPS+miR-200c-3p and LPS+AgPEI group (Figure 4A–D). All the above results indicated that the delivery of miR-200c-3p via Lipo-AgPEI-miR-200c-3p could more effectively inhibit the LPS-induced inflammatory response in ATDC5 cells.

OA progression involves severe cartilage destruction and lesions on the joint surface and degradation of cartilage extracellular matrix components. Whether Lipo-AgPEI-miR-200c-3p produces a protective effect on the cartilage extracellular matrix in ATDC5 cells is still unknown. Therefore, we assessed the effect of Lipo-AgPEI-miR-200c-3p on cartilage extracellular matrix components. The results showed that MMP3, MMP13, and ADAMTS-4 expressions were dramatically upregulated in ATDC5 cells following LPS stimulation, but Collagen II was significantly down-regulated. The expressions of Collagen II were increased while the levels of MMP3, MMP13, and ADAMTS-4 were reduced following transfection of miR-200c-3p with LPS or the addition of AgPEI. In comparison to the LPS+miR-200c-3p and the LPS+AgPEI group, the expressions of MMP3, MMP13 and ADAMTS-4 were further downregulated and those of Collagen II were further upregulated following the treatment with Lipo-AgPEI-miR-200c-3p (Figure 4E–I).

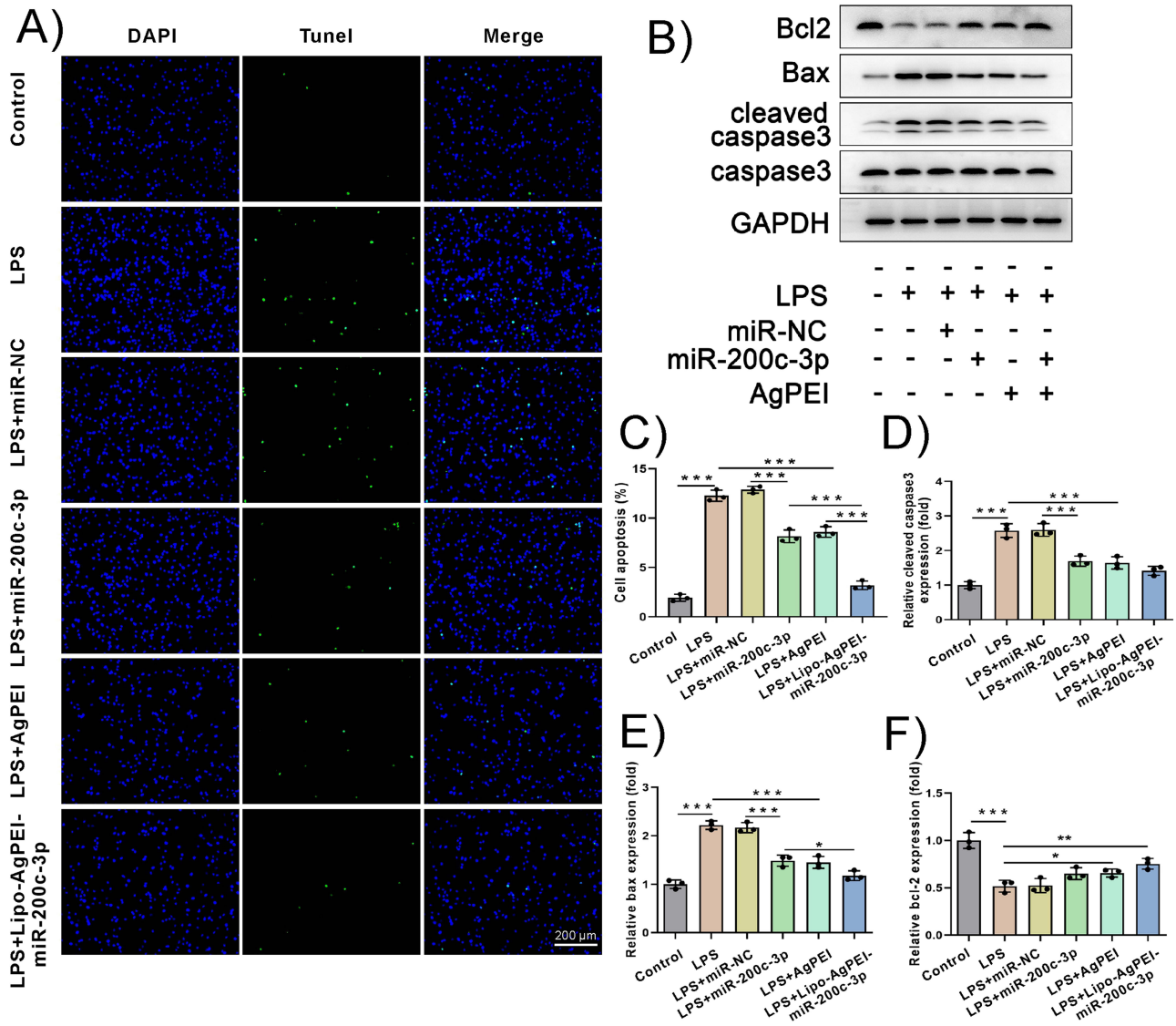

Figure 3 The effect of miR-200c-3p on ATDC5 cell apoptosis delivered by Lipo-AgPEI-miR-200c-3p. (**A**) The Tunel staining results (the green fluorescence presents apoptosis cells). (**B**) The expression of apoptosis-related proteins (Bcl-2, Bax, cleaved caspase3, caspase3) were detected by western blot. (**C**) The quantitative results of Tunel staining. (**D**–**F**) The quantitative analysis of Bcl-2, Bax, cleaved caspase3 in chondrocytes. The protein levels were normalized to the level of the internal control, GAPDH and presented as fold changes relative to the control group. Data are representative of three independent experiments and presented as means ± SD. Statistical significance was determined by one-way ANOVA. **P*<0.05, ***P* < 0.01, ****P* < 0.001.

miR-200c-3p Regulates ATDC5 Cell Function by Inhibiting ZEB2 Expression

We used three websites miRNA databases (TargetScan, miRDB, and miRWalk) to predict the target genes of miR-200c-3p. A Venn Diagram from an internet page was used to create the diagram (Figure 5A). Seven genes—ZEB2, GPM6A, EPS8, TFAP2A, PTPN21, ZEB1, and GOLGA7—were located near the intersection. To verify which gene played the key role in regulatory function, we first detected the expression of the above seven genes in the LPS-induced ATDC5 cell model, and RT-qPCR results showed that ZEB2 was significantly up-regulated in the LPS-induced ATDC5 cell model (Figure 5B).

Besides, we transfected miR-200c-3p into LPS-induced ATDC5 cells and the expression of ZEB2 was determined by RT-qPCR. The results demonstrated that ZEB2 expression was substantially down-regulated after the transfection of miR-200c-3p (Figure 5C). To further determine the relationship between miR-200c-3p and ZEB2, the double luciferase reporter gene experiment was performed (Figure 5D). ZEB2-WT vector and ZEB2-MUT vector were transfected with

https://doi.org/10.2147/IJN.S491711

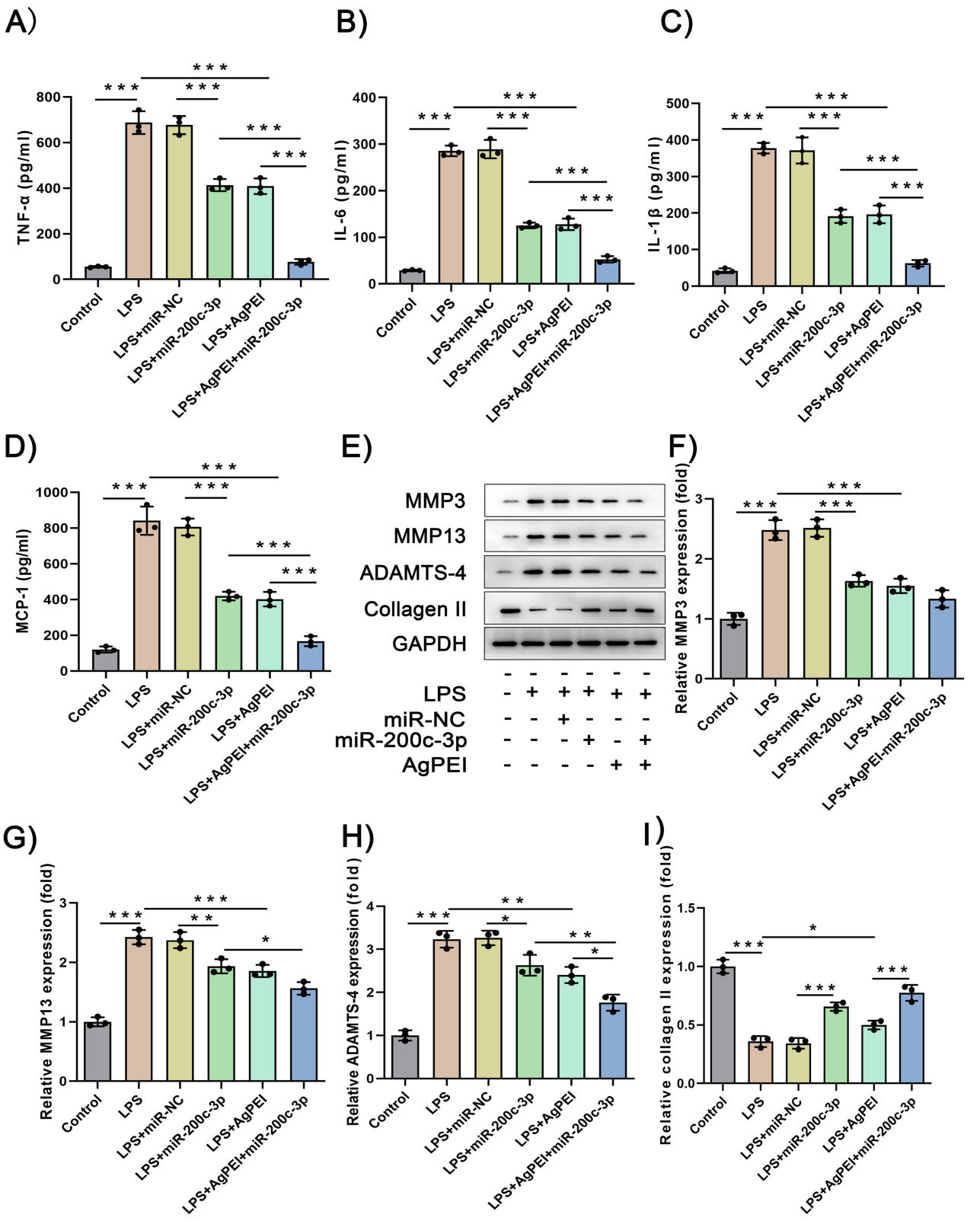

Figure 4 The Effect of miR-200c-3p on ATDC5 cells inflammatory and extracellular matrix metabolism. (**A-D**) The pro-inflammatory factors levels (TNF-α, IL-6, IL-1β and MCP-1) were determined by Elisa. (**E**) The expression of MMP3, MMP13, ADAMTS-4, Collagen II were detected by western blot. (**F–I**). The quantitative analysis of MMP3, MMP13, ADAMTS-4, Collagen II in chondrocytes. The protein levels were normalized to the level of the internal control, GAPDH and presented as fold changes relative to the control group. Data are representative of three independent experiments and presented as means ± SD. Statistical significance was determined by one-way ANOVA. **P*<0.05, ***P*< 0.01, ****P*< 0.001.

 https://doi.org/10.2147/IJN.S491711

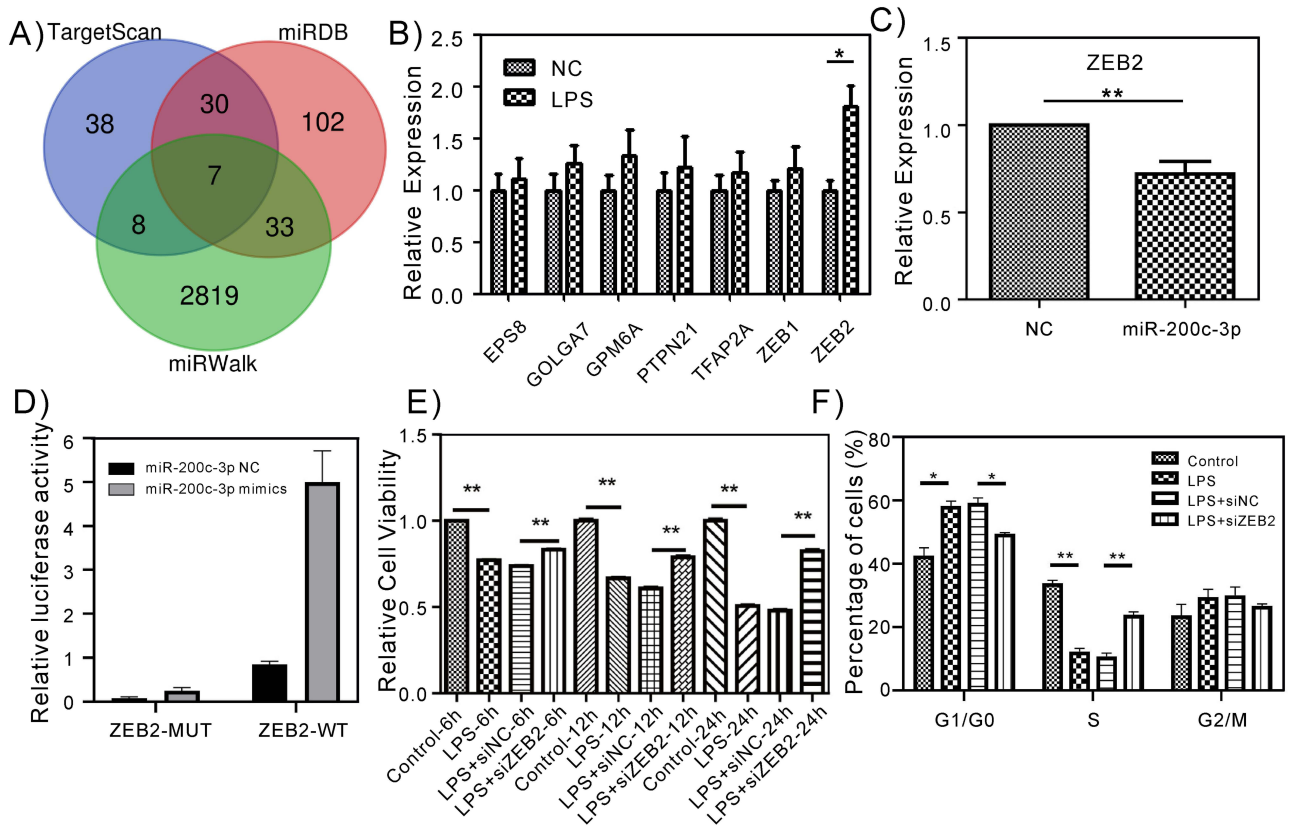

Figure 5 miR-200c-3p regulates mouse ATDC5 cell function by inhibiting ZEB2 expression. (**A**) The target gene of miR-200c-3p was found in the database. (**B**) The expression levels of EPS8, GOLGA7, GPM6A, PTPN21, TFAP2A, ZEB1 and ZEB2 were detected in LPS-induced ATDC5 cells. (**C**) After transfecting the miR-200c-3p, the expression level of ZEB2 was detected. (**D**) The results of the double luciferase reporter gene experiment suggest that miR-200c-3p binds to ZEB2. (**E**) Impact of varying ZEB2 knockdown times on ATDC5 cell viability. (**F**) The effect of ZEB2 knockdown on ATDC5 cell cycle was detected by flow cytometry. Statistical significance was determined by one-way ANOVA. **P*<0.05, ***P*< 0.01.

miR-200c-3p or miR-NC. The luciferase reporter gene results showed that the luciferase activity in the ZEB2-WT group was significantly increased, while no significant change in the ZEB2-MUT group.

Subsequently, we designed ZEB2 siRNA to knock down ZEB2 in LPS-induced ATDC5 cells, the cell proliferation and cell cycle changes were detected. The results showed that compared with the control group, the proliferation capacity of ATDC5 cells was significantly increased after ZEB2 knockdown (Figure 5E). In addition, the percentage of ATDC5 cells in the G0/G1 phase was significantly decreased, while the percentage of ATDC5 cells in the S phase was significantly increased (Figure 5F).

ZEB2 Plays a Key Role in Chondrocyte Apoptosis, Inflammation, Cartilage Matrix Synthesis and Catabolism

To further investigate the effect of ZEB2 on chondrocyte apoptosis, we detected apoptosis rates and apoptosis-related protein levels in ATDC5 cells. Flow cytometry results showed knockdown ZEB2 significantly reversed chondrocyte apoptosis in LPS-induced osteoarthritis cell models (Figure 6A–B). The western blot results demonstrated that the expression levels of cleaved caspase3, Bax and cleaved caspase3 were significantly decreased when knockdown ZEB2 (Figure 6C–E). Besides, the pro-inflammatory factors (TNF-α, IL-6, IL-1β and MCP-1) expressions and the chondro-catabolic related proteins (MMP3, MMP13, MMP13) also were detected. The results revealed there was significantly decreased in pro-inflammatory factors (TNF-α, IL-6, IL-1β, and MCP-1) (Figure 7A–D) and the expression levels of cartilage catabolic associated proteins (MMP3, MMP13, ADAMTS-4) after knockdown ZEB2. The Collagen II expression was significantly increased inversely (Figure 7E–I). All above results suggested that ZEB2 could induce chondrocyte apoptosis, inflammation and promote cartilage degradation.

https://doi.org/10.2147/IJN.S491711

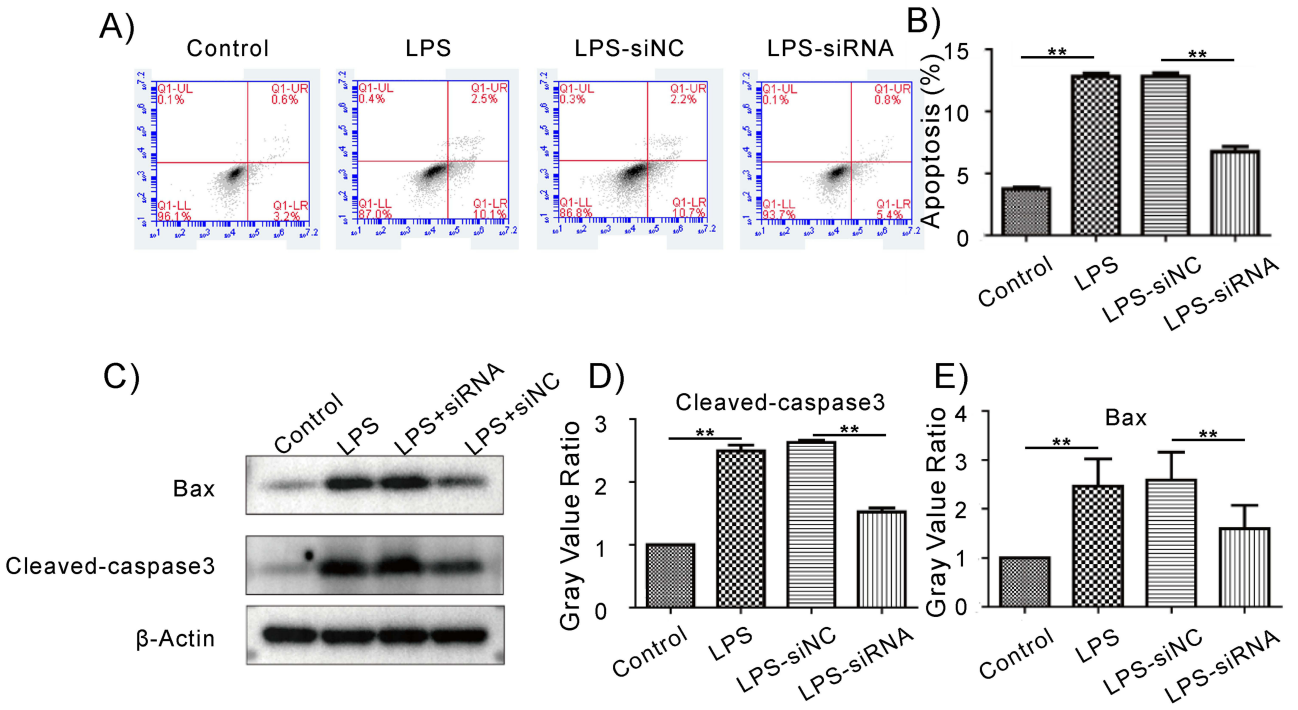

Figure 6 The Effect of ZEB2 on ADTC5 Cell apoptosis. The ADTC5 cells were pre-transfected with si-ZEB2 and then stimulated with LPS. (**A**) ATDC5 cell apoptosis was detected by flow cytometry. (**B**) The quantitative analysis of chondrocyte apoptosis. (**C**) The apoptosis-related protein (Bax and Cleaved-caspase3) expressions were detected by western blot. (**D**–**E**) The quantitative analysis of Bax and Cleaved-caspase3 in chondrocytes. The protein levels were normalized to the level of the internal control, β-actin and presented as fold changes relative to the control group. Data are representative of three independent experiments and presented as means ± SD. Statistical significance was determined by one-way ANOVA. $^{**}P < 0.01$.

Discussion

Clinically, joint injuries and intra-articular fractures often cause damage to the articular cartilage, which may evolve into OA when not treated well. We designed engineered miR-200c-3p nanoparticles and stimulated ADTC5 cells with LPS to investigate the role of miR-200c-3p nanoparticles in antagonizing chondrocyte inflammation, apoptosis, and matrix degradation.

PEI, with good gene-carrying ability, could evade lysosomal lysis and digestion, has been widely studied in the application of gene vectors and gene drugs.[39] Silver ions synthesize cleavable chemical bonds with branched-chain polyethylenimine B-PEI to form nanoscale-scale large-molecular-weight PEIs by the action of carrying a positive charge, increasing the amount of PEI-carrying gene fragments.[40] After being engulfed into the cell, the chemical bond between silver ion and B-PEI is easily cleaved and degraded into small molecular weight B-PEI and trace amounts of Ag, which reduces the toxicity of the material. In inflammatory environments, the cellular microenvironment tends to be acidic,[41] and nanoscale AgPEI-miR-200c-3p is prone to charge reversal, resulting in self-allosterism or partial dissociation, and easy released target genes. Electron microscopy detection found that the size of miR-200c-3p did not increase significantly after adsorption to the surface of AgPEI particles, and the particle size of the synthesized AgPEI-miR -200c-3p nanoparticles did not significantly increase compared with that of AgPEI. After miR-200c-3p adsorbed on the surface of AgPEI nanoparticles, it reduced the hydration radius of PEI chains, which was conducive to the endocytosis of cells. In the experiment, the zeta potential of AgPEI-miR-200c-3p was significantly lower than that of AgPEI, and the zeta potential of lipid nanoparticles Lipo-AgPEI-miR-200c-3p was lower and nearly neutral, which made Lipo-AgPEI-miR-200c-3p facilitate the escape of lysosomes after entering the cell. It can be seen from the results of cell viability assay that the cytotoxicity was reduced after the complexation of B-PEI and Ag, while the cytotoxicity was not significantly different from that of the AgPEI group after miR-200c-3p loading, while the cytotoxicity of AgPEI-miR -200c-3p after liposome encapsulation was significantly different from that between the Ag group and the PEI group,

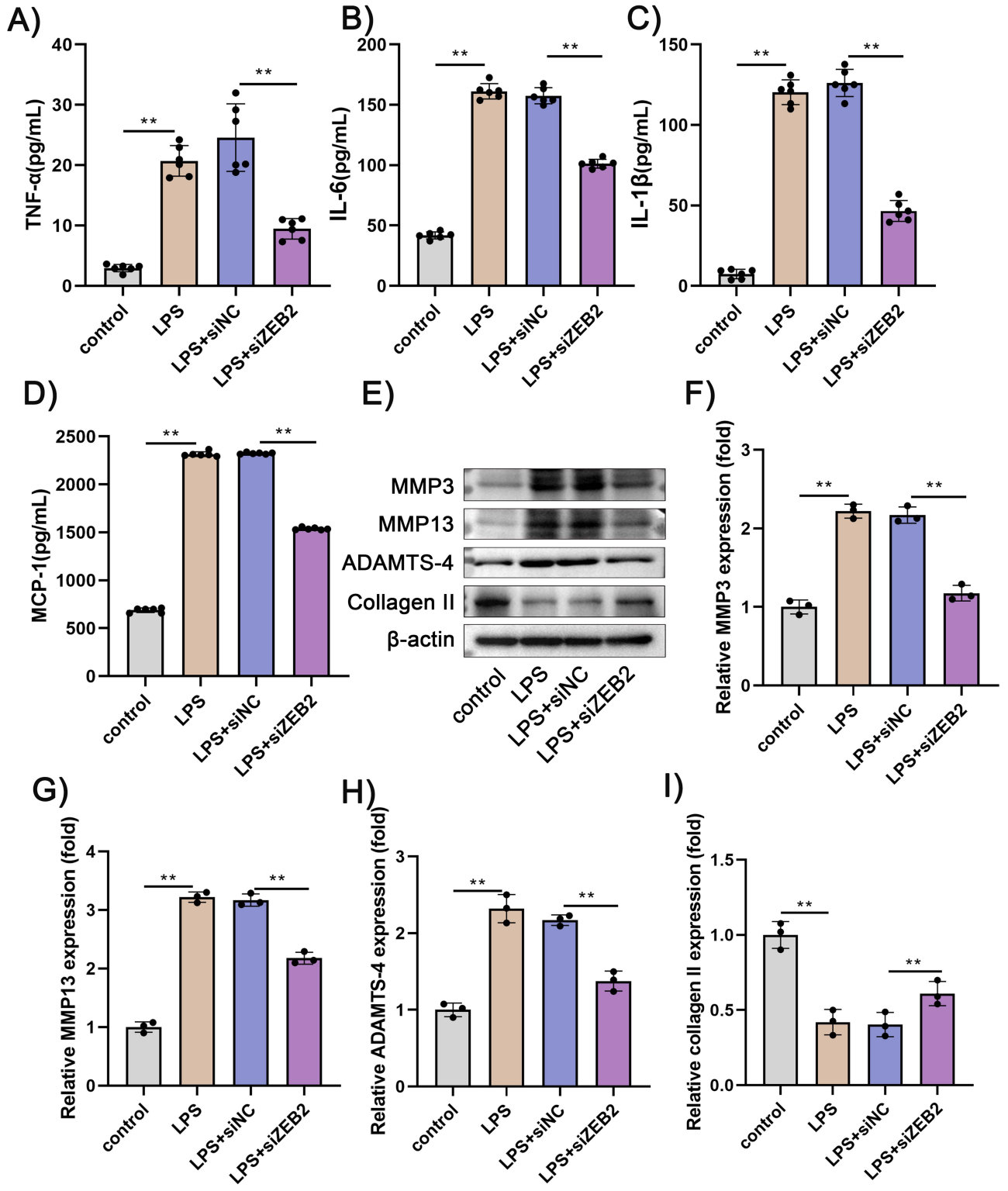

Figure 7 The expressions of relative proteins. The ADTC5 cells were pre-transfected with si-ZEB2 and then stimulated with LPS, the content of TNF-α, IL-6, IL-1β and MCP-1 in ATDC5 cells were determined by Elisa (**A**–**D**). (**E**). The expression of MMP3, MMP13, ADAMTS-4, Collagen II were detected by western blot. (**F**–**I**). The quantitative analysis of MMP3, MMP13, ADAMTS-4, Collagen II in chondrocytes. The protein levels were normalized to the level of the internal control, GAPDH and presented as fold changes relative to the control group. Data are representative of three independent experiments and presented as means ± SD. Statistical significance was determined by one-way ANOVA. ***P*< 0.01.

https://doi.org/10.2147/IJN.S491711

indicating that the cytotoxicity of Ag and PEI alone could be improved after liposome encapsulation. This is related to the hydrophilic and degradable properties of PEG in the liposomes, and neutralize the surface charge of the material.

Liposomes and cholesterol synthesize microvesicles, which are often used to encapsulate drugs for drug delivery and sustained release.[42] After the liposomes synthesized by microfluidic technology encapsulated AgPEI-miR-200c-3p, the particle size of the complex Lipo-AgPEI-miR-200c-3p was still maintained at 50~150nm. The results of differential scanning calorimetry showed that the phase transformation and dissociation of Lipo-AgPEI-miR-200c-3p synthesized by microfluidic technology at temperatures of nearly 37 °C and higher could release the encapsulated drugs. At the same time, the particle size test of up to 12 weeks also showed that the synthetic liposomes had good particle size dispersion and could be stored for a long time, which could make the long-term slow release of miR-200c-3p during actual use, reduce cytotoxicity and increase the action time of the drug.

Extensive loss of extracellular matrix (ECM) in articular cartilage is one of the pathological features of OA.[43] Reducing the degradation of ECM could inhibit the progression of OA. ECM is mainly composed of collagen and proteoglycan, among which collagen II is the main component of extracellular matrix.[44] Type II collagen fibers of normal tissue have a network half-life of several years and are therefore particularly stable. However, matrix metalloproteinases (MMPs) are significantly increased in osteoarthritis cartilage, and MMPs could hydrolyze a variety of extracellular matrix components (such as collagen, fibronectin and proteoglycan) and accelerate cartilage degeneration.[45] Relevant studies have shown that both MMP-3 and MMP-13 in the MMPs family are abnormally expressed and play an important role in the occurrence and development of OA disease.[46,47] The most well-known member of the polyproteinase family (ADAMTS), ADAMTS-4, is crucial for the breakdown of extracellular matrix polyproteinoglycans in addition to matrix metalloproteinases.[48]

ZEB2, a transcription factor, and studies have shown that ZEB2 can inhibit the expression of E-cadherin in epithelial cells, thereby promoting the epithelial-mesenchymal transition of tumors and accelerating cancer progression.[49–51] The expression of miR-200c-3p was significantly down-regulated in inflammatory breast cancer, while the expression of ZEB2 was significantly up-regulated.[52] It has also been shown that miR-200c-3p could bind to ZEB2 in prostate cancer cell lines (PC3 and DU145) to inhibit the development and progression of prostate cancer.[53] Compared with the control group, the proliferation ability of ATDC5 cells increased significantly, the percentage of ATDC5 cells in G0/G1 phase decreased, the percentage of cells in S phase increased significantly, and its apoptosis decreased significantly, indicating that ZEB2 had the functions of inhibiting ATDC5 cell proliferation, slowing down the cell cycle progression, and promoting apoptosis. In addition, inflammatory infiltration and degradation of cartilage matrix are also important pathological manifestations of osteoarthritis, and after knockdown of ZEB2 in the LPS-induced osteoarthritis cell model, chondrocyte inflammation and cartilage matrix catabolism were significantly blocked, while cartilage matrix anabolism was significantly promoted, indicating that ZEB2 could promote cartilage catabolism and inflammation and inhibit cartilage anabolism.

We also note that there are shortcomings in this study. Lipo-AgPEI-miR-200c-3p nanoparticles play a role in LPS-mediated chondrocyte inflammation, apoptosis and matrix degradation. However, further research is needed on whether Lipo-AgPEI-miR-200c-3p nanoparticles play vital role in other models of OA cells, such as IL-1β-mediated and TNF-α-mediated OA models of chondrocytes. Besides, the mechanism of miR-200c-3p targeting ZEB2 to regulate the anti-inflammatory and anti-apoptotic effects has not been verified in OA patients' chondrocytes. Furthermore, the animal experimental part has not been completed to verify the role of drug delivery system of AgPEI-miR-200c-3p. It remains to be further explored how to make Lipo-AgPEI-miR-200c-3p have targeted aggregation and repair effects on cartilage damage and inflammation in animal OA models and be safe and non-toxic, so as to truly achieve clinical transformation.

Conclusion

In this paper, the nanoliposome particles Lipo-AgPEI-miR-200c-3p synthesized by microfluidic chip could decrease the cytotoxicity of delivered gene materials and achieve good physicochemical properties of drugs. Following LPS stimulation, AgPEI and miR-200c-3p can both increase cell survival, inhibit cell apoptosis, and lower the expression levels of TNF-α, IL-6, IL-1β, and MCP-1 proteins in mouse ADTC5 cells. MMP3, MMP13, and ADAMTS-4 expression was downregulated whereas collagen II expression was upregulated. Furthermore, Lipo-AgPEI-miR-200c-3p can improve the biological effect and better perform the synergistic role of AgPEI and miR-200c-3p. We investigated the relationship between miR-200c-3p and the downstream target gene ZEB2 in ATDC5 cells, revealing the potential of the miR-200c-

3p/ZEB2 axis may be a therapeutic target for OA. These results suggest that miR-200c-3p regulates the inflammatory response, apoptosis, and matrix degradation of chondrocytes during osteoarthritis by targeting ZEB2. Overall, this study identified the interaction between miR-200c-3p and its downstream target gene ZEB2, providing a basis for finding new targets for OA therapy.

Data availability

The datasets used in the present study are available from the corresponding authors on reasonable request.

Author Contributions

All authors made a significant contribution to the work reported, whether that is in the conception, study design, execution, acquisition of data, analysis and interpretation, or in all these areas; took part in drafting, revising or critically reviewing the article; gave final approval of the version to be published; have agreed on the journal to which the article has been submitted; and agree to be accountable for all aspects of the work.

Funding

This work was supported by the National Natural Science Foundation of China (22204009), the Natural Science Foundation of the Jiangsu Higher Education Institution of China (22KJB150019), State Key Laboratory of Analytical Chemistry for Life Science (SKLACLS2315), Changzhou Science & Technology Program (CJ20220125), the Changzhou Science and Technology Bureau (WZ202204), Changzhou No. 2. People's Hospital Foundation (2022K004).

Disclosure

The authors declare no competing financial interest.

References

1. Jiang Y. Osteoarthritis year in review 2021: biology. *Osteoarth Cartil*. 2022;30(2):207–215. doi:10.1016/j.joca.2021.11.009
2. Martel-Pelletier J, Barr AJ, Cicuttini FM, et al.. Osteoarthritis. *Nat Rev Dis Primers*. 2016;2:1. doi:10.1038/nrdp.2016.72
3. Chen D, Shen J, Zhao W, et al.. Osteoarthritis: toward a comprehensive understanding of pathological mechanism. *Bone Res*. 2017;5(1):16044. doi:10.1038/boneres.2016.44
4. Glyn-Jones S, Palmer AJR, Agricola R, et al.. Osteoarthritis. *Lancet*. 2015;386(9991):376–387. doi:10.1016/S0140-6736(14)60802-3
5. Robinson WH, Lepus CM, Wang Q, et al.. Low-grade inflammation as a key mediator of the pathogenesis of osteoarthritis. *Nat Rev Rheumatol*. 2016;12(10):580–592. doi:10.1038/nrrheum.2016.136
6. Bannuru RR, Osani MC, Vaysbrot EE, et al.. OARSI guidelines for the non-surgical management of knee, hip, and polyarticular osteoarthritis. *Osteoarth Cartil*. 2019;27(11):1578–1589. doi:10.1016/j.joca.2019.06.011
7. Fujii Y, Liu L, Yagasaki L, Inotsume M, Chiba T, Asahara H. Cartilage Homeostasis and Osteoarthritis. *Int J Mol Sci*. 2022;23(11):6316. doi:10.3390/ijms23116316
8. Evans CH, Ghivizzani SC, Robbins PD. Osteoarthritis gene therapy in 2022. *Curr Opin Rheumatol*. 2023;35(1):37–43. doi:10.1097/BOR.0000000000000918
9. Pouton CW, Seymour LW. Key issues in non-viral gene delivery. *Adv Drug Deliv Rev*. 2001;46:187–203. doi:10.1016/S0169-409X(00)00133-2
10. Foldvari M, Chen DW, Nafissi N, Calderon D, Narsineni L, Rafiee A. Non-viral gene therapy: gains and challenges of non-invasive administration methods. *J Control Release*. 2016;240:165–190. doi:10.1016/j.jconrel.2015.12.012
11. Pack DW, Hoffman AS, Pun S, Stayton PS. Design and development of polymers for gene delivery. *Nat Rev Drug Discov*. 2005;4(7):581–593. doi:10.1038/nrd1775
12. Vickers KC, Palmisano BT, Shoucri BM, Shamburek RD, Remaley AT. MicroRNAs are transported in plasma and delivered to recipient cells by high-density lipoproteins. *Nat Cell Biol*. 2011;13(4):423–433. doi:10.1038/ncb2210
13. Kamiya H, Tsuchiya H, J. Y, H. H. Intracellular trafficking and transgene expression of viral and non-viral gene vectors. *Adv Drug Deliv Rev*. 2001;52:153–164. doi:10.1016/S0169-409X(01)00216-2
14. Sung YK, Kim SW. Recent advances in the development of gene delivery systems. *Biomater Res*. 2019;23:8. doi:10.1186/s40824-019-0156-z
15. Yin H, Kanasty RL, Eltoukhy AA, Vegas AJ, Dorkin JR, Anderson DG. Non-viral vectors for gene-based therapy. *Nat Rev Genet*. 2014;15(8):541–555. doi:10.1038/nrg3763
16. Yan Y, Liu XY, Lu A, Wang XY, Jiang LX, Wang JC. Non-viral vectors for RNA delivery. *J Control Release*. 2022;342:241–279. doi:10.1016/j.jconrel.2022.01.008
17. Miller JB, Zhang S, Kos P, et al.. Non-viral CRISPR/cas gene editing in vitro and in vivo enabled by synthetic nanoparticle co-delivery of Cas9 mRNA and sgRNA. *Angew Chem Int Ed Engl*. 2017;56(4):1059–1063. doi:10.1002/anie.201610209
18. Tseng YC, Mozumdar S, Huang L. Lipid-based systemic delivery of siRNA. *Adv Drug Deliv Rev*. 2009;61(9):721–731. doi:10.1016/j.addr.2009.03.003

19. Lv S, Jing R, Liu X, et al.. One-step microfluidic fabrication of multi-responsive liposomes for targeted delivery of doxorubicin synergism with photothermal effect. *Int J Nanomed*. 2021;16:7759–7772. doi:10.2147/IJN.S329621
20. Bartel DP. MicroRNAs genomics, review biogenesis, mechanism, and function.pdf>. *Cell*. 2004;116:281–297. doi:10.1016/S0092-8674(04)00045-5
21. Bartel DP. MicroRNAs: target recognition and regulatory functions. *Cell*. 2009;136(2):215–233. doi:10.1016/j.cell.2009.01.002
22. Sercombe L, Veerati T, Moheimani F, Wu SY, Sood AK, Hua S. Advances and challenges of liposome assisted drug delivery. *Front Pharmacol*. 2015;6:286. doi:10.3389/fphar.2015.00286
23. Zhu Y, Shen R, Vuong I, et al.. Multi-step screening of DNA/lipid nanoparticles and co-delivery with siRNA to enhance and prolong gene expression. *Nat Commun*. 2022;13(1):4282. doi:10.1038/s41467-022-31993-y
24. He L, Hannon GJ. MicroRNAs: small RNAs with a big role in gene regulation. *Nat Rev Genet*. 2004;5(7):522–531. doi:10.1038/nrg1379
25. Duan L, Liang Y, Xu X, Xiao Y, Wang D. Recent progress on the role of miR-140 in cartilage matrix remodelling and its implications for osteoarthritis treatment. *Arthritis Res Ther*. 2020;22(1):194. doi:10.1186/s13075-020-02290-0
26. Luo C, Liang JS, Gong J, et al.. The function of microRNA-34a in osteoarthritis. *Bratisl Lek Listy*. 2019;120(5):386–391. doi:10.4149/BLL_2019_063
27. Sun Y, Kang S, Pei S, Sang C, Huang Y. MiR93-5p inhibits chondrocyte apoptosis in osteoarthritis by targeting lncRNA CASC2. *BMC Musculoskelet Disord*. 2020;21(1):26. doi:10.1186/s12891-019-3025-y
28. Chen H, Ye T, Hu F, et al.. Urchin-like ceria nanoparticles for enhanced gene therapy of osteoarthritis. *Sci Adv*. 2023;9(24):eadf0988. doi:10.1126/sciadv.adf0988
29. Klicka K, Grzywa TM, Mielniczuk A, Klinke A, Wlodarski PK. The role of miR-200 family in the regulation of hallmarks of cancer. *Front Oncol*. 2022;12:965231. doi:10.3389/fonc.2022.965231
30. Frangos T, Maret W. Zinc and cadmium in the aetiology and pathogenesis of osteoarthritis and rheumatoid arthritis. *Nutrients*. 2020;13(1):53. doi:10.3390/nu13010053
31. Li Z, Peng Y, Pang X, Tang B. Potential therapeutic effects of Mg/HCOOH metal organic framework on relieving osteoarthritis. *ChemMedChem*. 2020;15(1):13–16. doi:10.1002/cmdc.201900546
32. Guo D, Zhu L, Huang Z, et al.. Anti-leukemia activity of PVP-coated silver nanoparticles via generation of reactive oxygen species and release of silver ions. *Biomaterials*. 2013;34(32):7884–7894. doi:10.1016/j.biomaterials.2013.07.015
33. De Matteis V, Malvindi MA, Galeone A, et al.. Negligible particle-specific toxicity mechanism of silver nanoparticles: the role of Ag+ ion release in the cytosol. *Nanomedicine*. 2015;11(3):731–739. doi:10.1016/j.nano.2014.11.002
34. Hwang ET, Lee JH, Chae YJ, et al.. Analysis of the toxic mode of action of silver nanoparticles using stress-specific bioluminescent bacteria. *Small*. 2008;4(6):746–750. doi:10.1002/smll.200700954
35. Yang EJ, Kim S, Kim JS, Choi IH. Inflammasome formation and IL-1β release by human blood monocytes in response to silver nanoparticles. *Biomaterials*. 2012;33(28):6858–6867. doi:10.1016/j.biomaterials.2012.06.016
36. Yang Y, Guo L, Wang Z, et al.. Targeted silver nanoparticles for rheumatoid arthritis therapy via macrophage apoptosis and Re-polarization. *Biomaterials*. 2021;264:120390. doi:10.1016/j.biomaterials.2020.120390
37. Yang K, Ni M, Xu C, et al.. Microfluidic one-step synthesis of a metal−organic framework for osteoarthritis therapeutic microRNAs delivery. *Front Bioeng Biotechnol*. 2023;11:1239364. doi:10.3389/fbioe.2023.1239364
38. Xu C, Ni S, Zhuang C, et al.. Polysaccharide from Angelica sinensis attenuates SNP-induced apoptosis in osteoarthritis chondrocytes by inducing autophagy via the ERK1/2 pathway. *Arthritis Res Ther*. 2021;23(1):47. doi:10.1186/s13075-020-02409-3
39. Casper J, Schenk SH, Parhizkar E, Detampel P, Dehshahri A, Huwyler J. Polyethylenimine (PEI) in gene therapy: current status and clinical applications. *J Control Release*. 2023;362:667–691. doi:10.1016/j.jconrel.2023.09.001
40. Koetz J. The effect of surface modification of gold nanotriangles for surface-enhanced raman scattering performance. *Nanomaterials*. 2020;10(11):2187. doi:10.3390/nano10112187
41. Hegde B, Bodduluri SR, Satpathy SR, et al.. Inflammasome-independent leukotriene B(4) production drives crystalline silica-induced sterile inflammation. *J Immunol*. 2018;200(10):3556–3567. doi:10.4049/jimmunol.1701504
42. Ewe A, Panchal O, Pinnapireddy SR, et al.. Liposome-polyethylenimine complexes (DPPC-PEI lipopolyplexes) for therapeutic siRNA delivery in vivo. *Nanomedicine*. 2017;13(1):209–218. doi:10.1016/j.nano.2016.08.005
43. Rahmati M, Nalesso G, Mobasheri A, Mozafari M. Aging and osteoarthritis: central role of the extracellular matrix. *Ageing Res Rev*. 2017;40:20–30. doi:10.1016/j.arr.2017.07.004
44. Hodgkinson T, Kelly DC, Curtin CM, O'Brien FJ. Mechanosignalling in cartilage: an emerging target for the treatment of osteoarthritis. *Nat Rev Rheumatol*. 2022;18(2):67–84. doi:10.1038/s41584-021-00724-w
45. Hu Q, Ecker M. Overview of MMP-13 as a promising target for the treatment of osteoarthritis. *Int J Mol Sci*. 2021;22:4.
46. Wan Y, Li W, Liao Z, Yan M, Chen X, Tang Z. Selective MMP-13 inhibitors: promising agents for the therapy of osteoarthritis. *Curr Med Chem*. 2020;27(22):3753–3769. doi:10.2174/0929867326666181217153118
47. Wan J, Zhang G, Li X, et al.. Matrix metalloproteinase 3: a promoting and destabilizing factor in the pathogenesis of disease and cell differentiation. *Front Physiol*. 2021;12:663978. doi:10.3389/fphys.2021.663978
48. Mead TJ, Apte SS. ADAMTS proteins in human disorders. *Matrix Biol*. 2018;71-72:225–239. doi:10.1016/j.matbio.2018.06.002
49. Gregory PA, Bert AG, Paterson EL, et al.. The miR-200 family and miR-205 regulate epithelial to mesenchymal transition by targeting ZEB1 and SIP1. *Nat Cell Biol*. 2008;10(5):593–601. doi:10.1038/ncb1722
50. Park SM, Gaur AB, Lengyel E, Peter ME. The miR-200 family determines the epithelial phenotype of cancer cells by targeting the E-cadherin repressors ZEB1 and ZEB2. *Genes Dev*. 2008;22(7):894–907. doi:10.1101/gad.1640608
51. Fardi M, Alivand M, Baradaran B, Farshdousti Hagh M, Solali S. The crucial role of ZEB2: from development to epithelial-to-mesenchymal transition and cancer complexity. *J Cell Physiol*. 2019;234(9):14783–14799. doi:10.1002/jcp.28277
52. Fahim SA, Abdullah MS, Espinoza-Sánchez NA, et al.. Inflammatory breast carcinoma: elevated microRNA miR-181b-5p and reduced miR-200b-3p, miR-200c-3p, and miR-203a-3p expression as potential biomarkers with diagnostic value. *Biomolecules*. 2020;10:7. doi:10.3390/biom10071059
53. Zhang J, Zhang H, Qin Y, et al.. MicroRNA-200c-3p/ZEB2 loop plays a crucial role in the tumor progression of prostate carcinoma. *Ann Transl Med*. 2019;7(7):141. doi:10.21037/atm.2019.02.40